58032

MESA-PENETRATING FRACTURES, FRACTURE MINERALOGY, AND PROJECTED FAULT TRACES AT PAJARITO MESA

17

by

David Vaniman and Steve Chipera

Geology/Geochemistry Group
Los Alamos National Laboratory

ABSTRACT

Earlier studies have suggested that the traces of the Rendija Canyon and Guaje Mountain faults project across Pajarito Mesa, based on the distributions of fracture abundances and apertures on mesas to the north. However, the only direct evidence for faulting found at Pajarito Mesa is near the Rendija Canyon fault projection, as fault offsets observed in trench TW5. Offsets in outcrop were found farther to the west, about 490 m (1600 ft) from a potential Mixed Waste Disposal Facility (MWDF) boundary. These fault offsets, generally down to the west where closest to the potential MWDF in trench TW5, may be related to the southern extension of the Rendija Canyon fault. Inferred fault offsets in the bottom of Threemile Canyon, just south of Pajarito Mesa, have an opposite sense of apparent offset (down to the east). These inferred fault offsets in the canyon bottom may instead represent irregular flow-unit topography within the tuff, unrelated to faulting, or they may represent secondary faulting related to a section of steeply east-dipping tuff stratigraphy to the NE on top of Pajarito Mesa. Regardless of these various interpretations, the absence of any evidence for Holocene offset in faults at the mesa top indicates that the MWDF site is not compromised by young faulting.

Studies of mesa-penetrating fractures along the southern edge of Pajarito Mesa show no concentration of abundant fractures or increase in fracture apertures associated with the previously inferred projections of the Rendija Canyon or Guaje Mountain faults. Fracture apertures increase to the west where fracture orientations are strongly oriented N17°E ± 15°. This interval of relatively wide and oriented fractures represents the potential MWDF locality.

Clay minerals are formed in soils at the mesa top and transported downward into deeper fractures. With few exceptions, clay transport is effectively stopped where these fractures pass into the nonwelded tuff at the mesa base, where such transport is diverted laterally over short distances into the more permeable layers of nonwelded tuff rather than moving farther downward. The mineralogic data suggest that fracture transport just above the nonwelded tuff can discharge fluids at the mesa base, but association of clays with halite indicates that evaporative concentration may prevent many solutes from escaping from the mesa: However, the evidence for this evaporation effect has been found only in those parts of the mesa to the east of the potential MWDF.

Received by ER-RPF
JUN 0 4 1998

10458

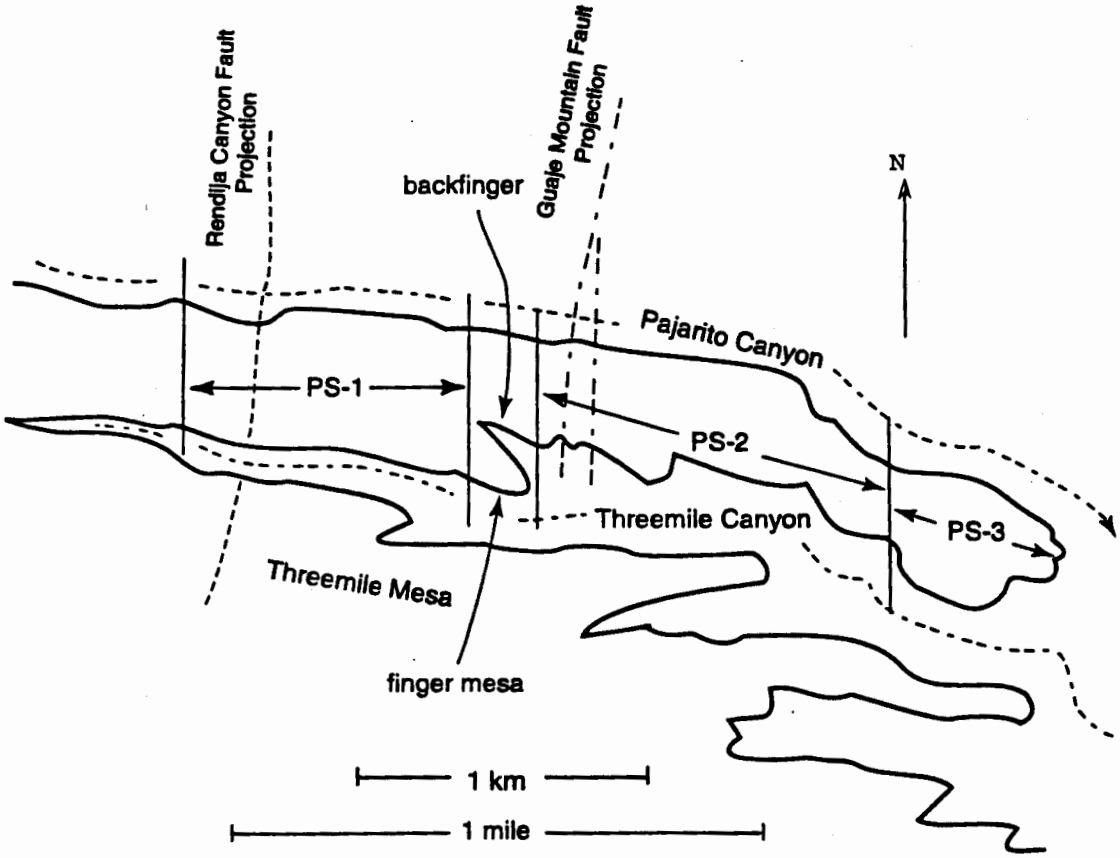

Fig. 1. Sketch map of Pajarito Mesa, showing the approximate boundaries of mesa segments considered as potential sites for mixed-waste disposal (PS-1, PS-2, and PS-3). Locations of the "finger mesa" and "backfinger" are also shown (see Figs. 3, 4, and text section on *Fracture Orientations*).

Two of the observable offsets are close together and relatively far to the west of PS-1, at the western margin of Plate 1:

- offset at New Mexico State Plane (NMSP) coordinates 1621438 E, 1765538 N. Plane of offset strikes N70°E, dips 86° SE. Measured displacement is 23 cm (9 in), down to the SE.
- offset at NMSP coordinates 1621513 E, 1765519 N. Plane of offset strikes N18°W, vertical dip. Inferred displacement is approximately 30 cm (12 in), down to the SW.

The third measured offset is closer to the western margin of PS-1 (490 m or 1600 ft, from the closest part of the potential MWDF facility outline; see Plate 1:

- offset at NMSP coordinates 1622300 E, 1765331 N. Plane of offset strikes N20°E, dips 77°SE. Measured displacement is 30 cm (12 in), down to the SE (this fault is shown on Plate 1).

Possible Fault Offsets in Threemile Canyon

Possible fault offsets of bedrock have also been found in Threemile Canyon, south of PS-1 between NMSP coordinates 1623450 E and 1624565 E; some of these possible offsets are shown at the southern edge of Plate 1. Inference of fault offset is based on anomalous reappearances of

the bottom of Threemile Canyon, south of Pajarito Mesa, could be caused by comparable secondary fault splays that curve to the SW. This interpretation can be reconciled with the steepened eastward slope of the surge at the base of unit 4 on the mesa top, NE of the down-to-the-east fault zone inferred here for the canyon bottom (see text by Reneau et al., this report). If this relationship is borne out, the strikes of the inferred canyon-bottom faults shown in Plate 1 may be more easterly than depicted.

As an alternative to either primary or secondary fault offsets in explanation of the irregularities in the unit 2/nonwelded tuff contact, it is possible that no fault offset occur in Threemile Canyon if these irregularities simply reflect undulatory relief in the surface of moderately-welded tuff unit 2. Such stratigraphic irregularities may be caused by irregular topography or irregular scouring between eruptive pulses in the Bandelier Tuff.

Without further information, and particularly without trenching in the bottom of Threemile Canyon, it is not prudent to attribute the repetition of contacts in the bottom of Threemile Canyon either to faulting or to unfaulted stratigraphic undulations. For the purposes of MWDF siting, the distinction between these two causes is not of regulatory concern because no Holocene fault offsets of any orientation were found in trenches along the mesa top.

Fault Offsets Observed in Mesa-Top Trenches: Relation to Previous Studies

Trench data collected on mesa tops to the north of Pajarito Mesa (TA-63; Kolbe et al., 1995) show no evidence of distinct fault breaks in the soil profiles above the tuff, where Vaniman and Wohletz (1990) projected the Guaje Mountain fault across Mesita del Buey. Trenching at Pajarito Mesa has shown that, as at Mesita del Buey, no young offsets along this projection are found on Pajarito Mesa (Kolbe et al., 1994).

The trace of the Rendija Canyon fault was also projected across Pajarito Mesa by Vaniman and Wohletz (1990). This projection crosses the mesa approximately where trenches TW5 and TW6 were subsequently excavated (see Plate 1). Preliminary results from trench-wall mapping indicate at least seven pre-Holocene faults in the eastern part of trench TW5, with offset down to the west. The age of this faulting is constrained by the unfaulted overlying soil horizons that lie beneath the pre-Holocene (50-60 ka) El Cajete pumice (Kolbe et al., 1994; Reneau et al., this report). Although the location of these fault offsets is close to the Rendija Canyon fault projection of Vaniman and Wohletz (1990), this does not necessarily indicate a "fix" on the location of the Rendija projection across Pajarito Mesa. The azimuths of these fault offsets are highly variable and they may represent the eastern portion of a broad zone of deformation, as suggested for both the Rendija Canyon and Guaje Mountain fault projections by Vaniman and Wohletz (1990) and suggested by sporadic fault offsets observed in outcrop to the west of the trenched zones on Pajarito Mesa (see section on *Observable Fault Offsets in Outcrop*, above). Regardless of the genesis and projections of the fault offsets observed in trench TW5 at Pajarito Mesa, the data obtained so far reveal no Holocene fault movement (Kolbe et al., 1994). This conclusion is of greatest importance for MWDF siting, for it indicates that the site will satisfy the provisions of 40 CFR 270, part 270.14, by directly indicating the absence of any Holocene fault movement.

FRACTURE DISTRIBUTIONS, ORIENTATIONS, AND APERTURES

Topographic maps with two-foot contour intervals were used to locate and measure 591 fractures along the generally well-exposed south margin of Pajarito Mesa. The north margin of the mesa was not mapped because of the poor exposure on north-facing slopes. Mapping concentrated on fractures that could be traced from the cliff-forming exposures of unit 3 into the underlying

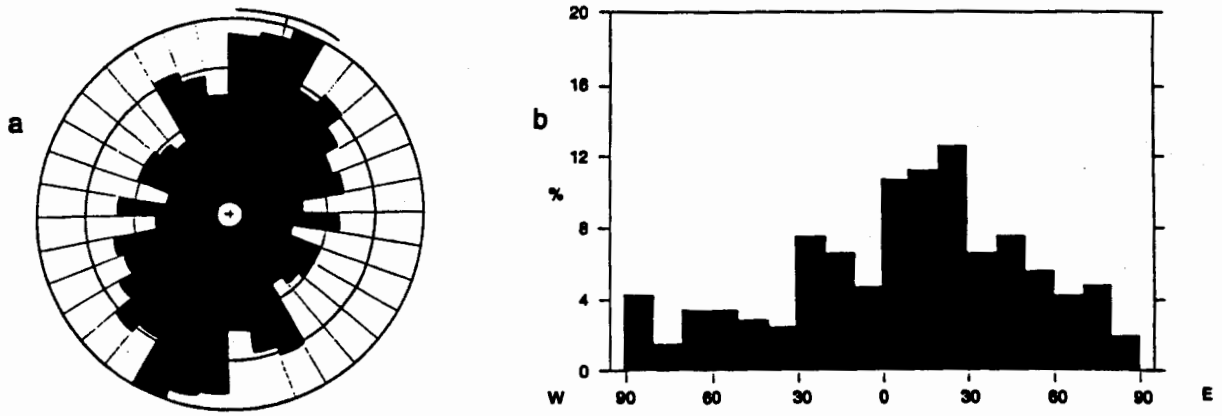

PS1	Statistics
N = 216 Class Interval = 10 degrees Maximum Percentage = 12.5 Mean Percentage = 5.56 Standard Deviation = 3.20	Vector Mean = 17.0 Conf. Angle = 15.36

Fig. 2. (a) Equal-area rose diagram for 216 fracture orientations at PS-1 (see Figure 1). Note strong preferred fracture orientation of N17°E. (b) Histogram of fracture orientations.

uncertainties. The prominent NNE fracture orientation in Fig. 3 is most similar to the fracture set of PS-1, whereas there is no apparent preferred orientation in Figure 4.

The fractures along PS-2 (Fig. 5) have no single prominent orientation, but instead are oriented in at least two sets: a broad distribution from N-S to N20°E and another cluster of approximately E-W orientation. Other orientations are common, weakening the prominence of any preferred orientation.

At PS-3 (Fig. 6) the fracture orientations are broadly isotropic. The commonest fracture orientations are NE and NW, and there appears to be a significant paucity of fractures trending E-W, but orientations are so broadly distributed that a larger data set would be needed to draw more detailed conclusions. Some of the scatter in fracture orientations at PS-3 may be attributed to the

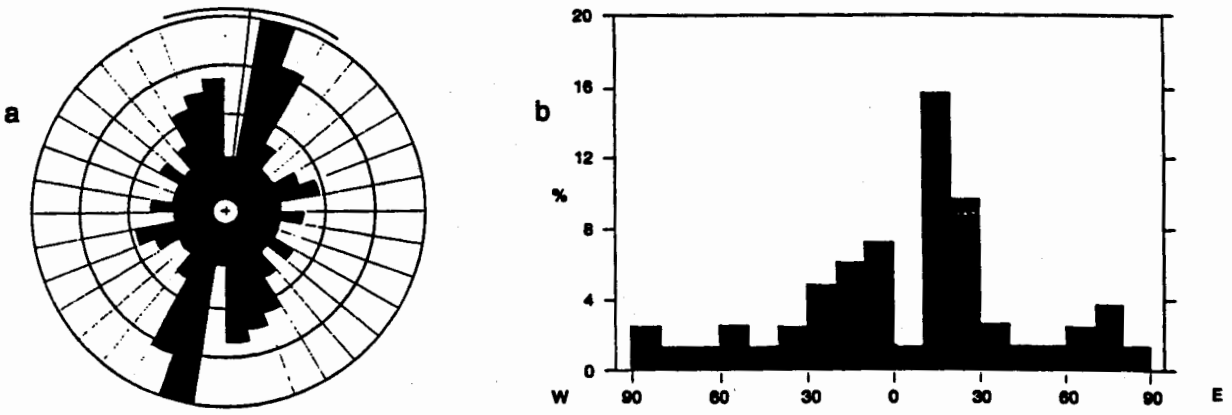

Finger Mesa	Statistics
N = 56 Class Interval = 10 degrees Maximum Percentage = 23.2 Mean Percentage = 5.56 Standard Deviation = 5.59	Vector Mean = 6.4 Conf. Angle = 24.78

Fig. 3. (a) Equal-area rose diagram for 56 fracture orientations along the finger mesa (see Figure 1). A prominent fracture set occurs at N10°E to N20°E, comparable to PS-1 (Figure 2). (b) Histogram of fracture orientations.

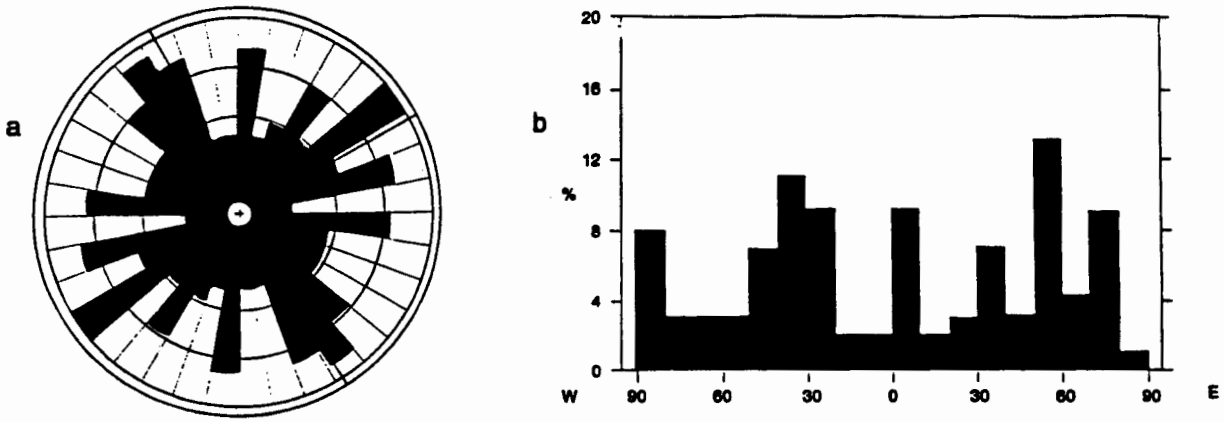

PS3	Statistics
N = 99 Class Interval = 10 degrees Maximum Percentage = 13.1 Mean Percentage = 5.56 Standard Deviation = 3.62	Vector Mean = 61.8 Conf. Angle = 477.66

Fig. 6. (a) Equal-area rose diagram for 99 fracture orientations at PS-3 (see Fig. 1). Note that the very broad scatter of fracture orientations leads to no confidence angle (>360°). Approximately 25% of the fractures measured for PS-3 occur on cliff faces of more N-S than E-W orientation; this may tend to reduce the number of N-S oriented fractures measured. Nevertheless, fractures of NW and NE orientation are more prominent than in other areas measured at Pajarito Mesa (see Fig. 7). (b) Histogram of fracture orientations.

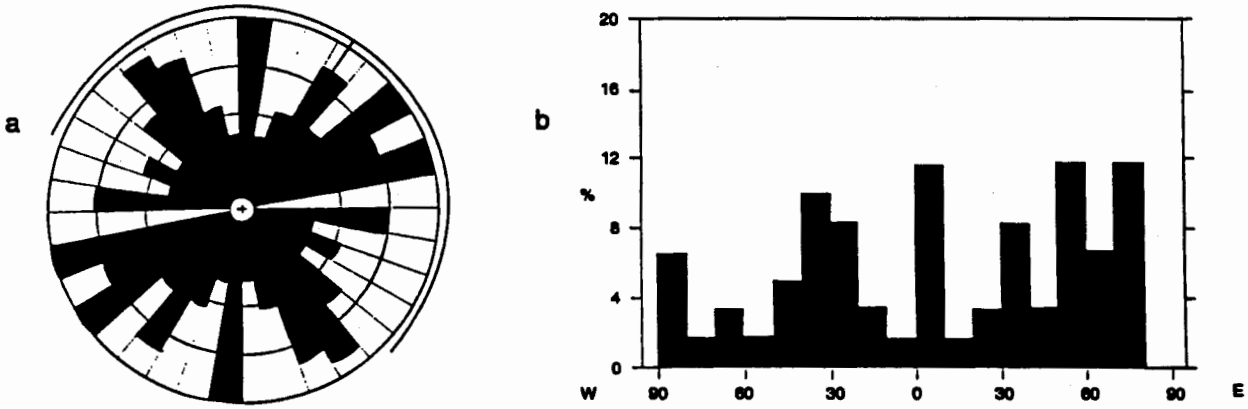

PS3, E-W cliffs	Statistics
N = 60 Class Interval = 10 degrees Maximum Percentage = 11.7 Mean Percentage = 5.88 Standard Deviation = 3.72	Vector Mean = 33.7 Conf. Angle = 100.88 R Magnitude = 0.103 Rayleigh = 0.5307

Fig. 7. Subset of 60 fractures measured from E-W trending cliffs at PS-3. (a) Equal-area rose diagram and (b) histogram of fracture orientations. Note that although the N-trending fractures are more prominent than they were in Fig. 6, the same general distribution of fracture orientations is observed.

Fracture Apertures

Fractures exposed at the mesa margin within tuff unit 3 are seldom sealed. Fractures tend to be open, with undulatory walls. Where fractures penetrate into the nonwelded tuffs underlying unit 3, they are not open but are instead filled with tuff detritus and clay; in some instances, fractures terminate in the nonwelded tuff and the clay from the fractures spreads laterally into small-scale sill-like features (see section below on *Petrologic/mineralogic evidence for possible barriers to*

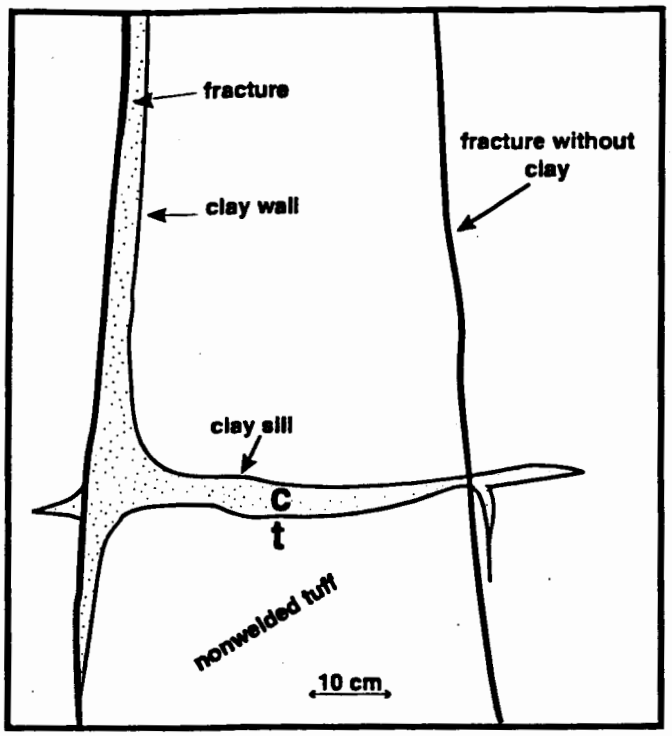

Fig. 9. Sketch showing dispersal of clay from mesa-penetrating fractures into horizontal substrata of nonwelded tuff, fracture F+192. Locations of clay-sill sample (c) and of unaltered tuff sample (t) are indicated, for comparison with the data for F+192 in Table 3.

FRACTURE MINERALOGY AND PETROGRAPHY

Mineral deposits within fractures are common at Pajarito Mesa, particularly in fractures exposed in trenches excavated in the mesa top and at the interface between welded and nonwelded tuffs at the break-in-slope at the bottom of the mesa-bounding unit 3 cliff. Table 2 summarizes the mineralogic data for 9 samples collected from trenches at the surface of Pajarito Mesa in areas PS-1 and PS-2; these trenches are shown in Plates 1 and 2 (trenches TW5, TW2, TE2, TE4, TE5, TE6, and TE8). Table 3 lists comparable data for samples from 17 fractures collected from the bottom of the mesa-bounding cliff along the southern margins of PS-1 and PS-2. The fracture-sample locations of Table 3 are also shown on Plates 1 and 2. Mineral abundances were determined by quantitative X-ray diffraction (QXRD). Sample preparation and analysis procedures are described in Broxton et al. (this report).

The commonest mineral filling in these fractures is smectite clay (up to 86%); this mineral is ubiquitous wherever mineral fillings occur in fractures. Lesser amounts of kaolinite and calcite occur with the smectite. Gypsum and halite are also found, notably in fracture samples at the bottom of the mesa-bounding cliff, providing evidence of evaporative processes that deserve particular mention. The smectite common to all fractures is more abundant in the shallow trench-exposed fractures (Table 2) than in the deeper fractures exposed in the cliff margins (Table 3). This reflects the more abundant illuviation of clay closer to the surface, with greater dilution of those minerals that represent tuff detritus (principally tridymite, cristobalite, quartz, and feldspar). The silica polymorphs in particular appear to reflect the composition of local tuffs. For instance, those near-surface fractures from trenches within unit 4 (all of the "TW" trenches in Table 2) have no detectable tridymite, in accord with the very low tridymite abundances in this unit (see Broxton et al., this report). In addition, the fractures at the mesa bottom in unit 3 have no detectable cristobalite, as observed in the immediately adjacent tuff, even though tuff samples from a few feet higher do contain cristobalite (Broxton et al., this report). The distributions of detrital minerals, especially of

TABLE 1. Fracture-Apertures for Cliff Margins

	PS-1	PS-2	PS-3
Number of fractures (n)	216	191	99
Mean aperture (cm)	3.4	1.9	2.3
Std. deviation (cm)	3.4	2.2	1.8
% fractures >2 cm	44%	18%	34%
% fractures >5 cm	15%	2%	5%
% fractures >10 cm	5%	1%	0

cristobalite, suggest little movement of tuff fragments within fractures despite the evidence for clay illuviation.

Early Hematite Alteration Along Some Fracture Walls

One fracture at the bottom of the mesa-bounding cliff (F+144) did not have a mineral filling but did have strongly reddened fracture walls; the mineralogic analysis of these reddened fracture walls is compared to the nonreddened, unaltered tuff in Table 3. The reddening is due to the development of dispersed hematite along the fracture wall, a type of alteration that appears to be part of the vapor-phase or fumarolic alteration that occurred soon after tuff emplacement. Hematite alteration of this nature is not representative of the current transport and alteration regime at Pajarito Mesa, whereas smectite formation and transport is.

Smectite Formation and Transport

Smectite is particularly abundant and common in the fractures along the mesa margin at PS-1. It appears to occur in more variable abundances in the fractures at PS-2, both on top of the mesa (samples from trenches TE-2 to TE-8, smectite abundances as low as 25%, Table 2) and at the bottom of the mesa-bounding cliff (samples from fractures of PS-2 commonly have smectite abundances of only 8-11%, Table 3). X-ray diffraction analysis of clay separates from both the trenches at the mesa top and the mesa-penetrating fractures show them to be strongly similar, suggesting that smectites form in the soil zone and are translocated into the fractures in the underlying tuff. Other studies have reached similar conclusions for trench samples (Davenport, 1993) based on illuviation structures in the shallow fracture-filling clays. Comparable illuviation features (e.g., cuspate-downward laminations) have been found in fractures at the base of the cliff, up to 15 m (50 ft) below the mesa top. Mineralogic similarities thus suggest that clay transport has occurred over ranges as great as 15 m (50 m), and perhaps farther, downward into Pajarito Mesa. The variation in clay illuviation depths suggests less particulate transport into deep fractures (>10 m or 33 ft) in the eastern part of the Pajarito Plateau than in the western part. This difference in clay illuviation may reflect differences in effective soil saturation at the mesa top, where the eastern mesa is characterized by an abundance of piñon-juniper-cactus vegetation and the western mesa supports abundant ponderosa pine. Alternatively, the decrease in fracture apertures in the eastern part of Pajarito Mesa (Fig. 8) may restrict transport by illuviation.

Petrologic/Mineralogic Evidence for Possible Barriers to Transport

Because the fractures mapped for this report are specifically those that are mesa-penetrating, it is possible to examine the presence or absence of any evidence for transport through the nonwelded interval at the base of the mesa. Figure 9 illustrates a feature commonly observed in the southern cliff margin of PS-2. Here the clay illuviation downward into mesa fractures penetrates a short distance into the nonwelded tuff before it is no longer able pass along the tightly sealed fracture trace. Clay penetration is then diverted away from the fracture and into thin substrata or lenses within the nonwelded unit. The clay-rich layers are seldom more than a few centimeters thick; the layers can not be traced laterally unless discolored by clay infiltration. This phenomenon indicates that there are sub-decimeter-scale substrata or lenses of greater permeability within the less permeable parts of the nonwelded tuffs. Because of the lack of any visible pre-alteration stratification in the adjacent nonwelded tuffs, it is possible that small differences in permeability caused by variable compaction may be the principal factor in determining whether or not the clays will infiltrate laterally into the tuff. This potential for small-scale permeability variations should be

ACKNOWLEDGMENTS

This work was funded by the Los Alamos National Laboratory Environmental Restoration Project as part of site characterization activities for the proposed Mixed Waste Disposal Facility. The authors thank Paul Aamodt, Darrell Bultman, Bob Gillis, Steven Reneau, David Broxton, Chuck Harrington, and Dean Nelson for their support; Doug Walther with FIMAD for map preparation; and Steven Reneau and John Wolff for reviews that helped to improve the manuscript.

REFERENCES

Broxton, D. E., Vaniman, D., Byers, F. M., Jr., Chipera, S. J., Kluk, E. C., and Warren, R. G., 1995, Stratigraphy, mineralogy and chemistry of befrock tuffs at Pajarito Mesa: this report.

Coppersmith, K. J., and Youngs, R. R., 1992, Modeling Fault Rupture Hazard for the Proposed Repository at Yucca Mountain, Nevada: *in* High Level Radioactive Waste Management, Proc. 3rd Ann. Conf., Las Vegas, Nevada, Amer. Nuc. Soc. and Amer. Soc. Civil Eng., p. 1142-1150.

Davenport, D. W., 1993, Micromorphology, Mineralogy, and Genesis of Soils and Fracture Fills on the Pajarito Plateau, New Mexico: Ph.D. Thesis, Texas Tech. Univ., Lubbock, 109 pp.

Kolbe, T., Sawyer, J., Gorton, A., Olig, S., Simpson, D., Fenton, C., Reneau, S., Carney, J., Bott, J., and Wong, I., 1994, Evaluation of the Potential for Surface Faulting at the Proposed Mixed Waste Disposal Facility, TA-67: unpublished report, Woodward-Clyde Federal Services, Oakland, California, 3 volumes.

Kolbe, T., Sawyer, J., Springer, J., Olig, S. ,Reneau, S., Hemphill-Haley, M., and Wong, I., 1995, Evaluation of the Potential for Surface Faulting at TA-63: unpublished report, Woodward Clyde Federal Services, Oakland, California.

Reneau, S. L., Kolbe, T., Simpson, D., Carney, J. S., Gardner, J. N., Olig, S. S., and Vaniman, D. T., 1995, Surficial materials and structure at Pajarito Mesa: this report.

Vaniman, D., and Wohletz, K., 1990. Results of Geological Mapping/Fracture Studies: TA-55 Area. Memo EES1-SH90-17. Amended in 1991 by Memo EES1-SH91-12; 50 pp, 1 plate

Contents

Introduction 1
by Steven L. Reneau and Robert Raymond, Jr.

Stratigraphy, Mineralogy and Chemistry of Bedrock Tuffs at Pajarito Mesa 5
by D. E. Broxton, D. Vaniman, F. M. Byers, Jr., S. J. Chipera, E. C. Kluk, and R. G. Warren

Surficial Materials and Structure at Pajarito Mesa 31
by Steven L. Reneau, Thomas R. Kolbe, David T. Simpson, John S. Carney, Jamie N. Gardner, Susan S. Olig and David T. Vaniman

Mesa-Penetrating Fractures, Fracture Mineralogy, and Projected Fault Traces at Pajarito Mesa 71
by David Vaniman and Steve Chipera

Potential Mesa-Edge Instability at Pajarito Mesa 87
by Steven L. Reneau